5-22-1989

Calcium Levels in Ruffle-Ended and Smooth-Ended Maturation Ameloblasts

S. H. Ashrafi
University of Illinois at Chicago

D. R. Eisenmann
University of Illinois at Chicago

A. E. Zaki
University of Illinois at Chicago

Recommended Citation

Utah State University
MERRILL-CAZIER LIBRARY

CALCIUM LEVELS IN RUFFLE-ENDED AND SMOOTH-ENDED MATURATION AMELOBLASTS

S. H. Ashrafi, D.R. Eisenmann[*] and A.E. Zaki

Department of Histology, College of Dentistry
University of Illinois at Chicago, Chicago, Illinois 60612

Abstract

Scanning electron microscopy was used to distinguish the topographical characteristics of two maturation ameloblast types in freeze-dried blocks of enamel organ tissue.   This distinction was based primarily upon the configuration of the distal ends of the ameloblasts and the presence or absence of wide intercellular spaces.

Energy dispersive x-ray spectrometry was applied to compare calcium levels in various regions of tissue identified as constituting either ruffle-ended or smooth ended ameloblasts.   Greater levels of calcium were found in the distal ends of the ruffle-ended cells than in their proximal ends. In addition, greater calcium levels were found in the distal ends of the ruffle-ended cells than the distal ends of the smooth-ended cells. The higher calcium levels in ruffle-ended cells correlates with the view that these cells are actively involved in control of movement of calcium to the enamel front.

[*]Address for correspondence:
Dale R. Eisenmann, Department of Histology, College of Dentistry, University of Illinois at Chicago, Chicago, Illinois 60612 Phone No. (312) 996-7732

Introduction

A rapid increase in mineral content of enamel occurs during the maturation stage of amelogenesis (Reith and Cotty, 1962; Hammarstrom, 1967; Robinson et al., 1979).   Much attention has been focused upon correlation of enamel mineralization patterns with the cyclic modulation of the two morphologic types of maturation ameloblasts (Suga, 1959; Warshawsky and Smith, 1974; Boyde and Reith, 1976, 1977; Josephsen and Fejerskov, 1977; Takano and Ozawa, 1980; Reith and Boyde, 1981; Skobe et al., 1985; Nishikawa and Josephsen, 1987; and Smith et al., 1987). Ruffle-ended maturation ameloblasts are thought to be more actively involved in transport of calcium from enamel organ tissue fluid to the adjacent mineralizing enamel because of their association with bands of greatest calcium reactivity in the surface of adjacent enamel (Reith and Boyde, 1981; Takano et al., 1982; Crenshaw and Takano, 1982; Reith et al., 1982; and McKee et al., 1987).   Mechanisms for this activity are not clear.   It has been suggested that ruffle-ended ameloblasts might control calcium transport by establishing a calcium gradient in the direction of the mineralizing enamel by means of membrane-associated components, carrier proteins, organelles or free cytosolic calcium (Crenshaw and Takano, 1982; Eisenmann et al., 1982; Reith, 1983; Taylor, 1984; Reith and Boyde, 1985; Kawamoto and Shimizu, 1987).

We have previously reported a gradient of calcium concentration increasing toward the distal end of the secretory ameloblast using energy dispersive x-ray spectrometry of freeze-dried enamel organ tissue (Eisenmann et al., 1984; and Ashrafi et al., 1987). Recently Takano et al. (1988) histochemically localized calcium-GBHA precipitates in maturation ameloblasts in association with various organelles including the ruffled border. Previously, little, if any information was available comparing calcium levels in ruffle-ended and smooth-ended ameloblasts. The aim of this study was to combine scanning electron microscopy (SEM) and energy dispersive x-ray spectrometry (EDX) of freeze-dried maturation enamel organ tissue to attempt to distinguish the topographical characteristics of the two maturation ameloblast types and determine if there are detectable differences in calcium levels between the ruffle-ended and smooth-ended ameloblasts

at their proximal and distal ends.

Materials and Methods

Nine male Sprague-Dawley rats weighing 100-150 grams were used in this investigation. Rats were killed by ether overdose and as quickly as possible incisors were partially separated from alveolar bone by manual dislocation (Eisenmann et al., 1984). This step caused a separation between the enamel organ tissue and the enamel surface at the ameloblast-enamel interface. This procedure was completed within approximately one minute after the death of the animal, and the incisor was then immediately frozen for 15 seconds in isopentane (-150°C), chilled with liquid nitrogen and then maintained in liquid nitrogen before freeze-drying. After freeze-drying at -35°C in a cryostat under vacuum for two days, regions of maturation ameloblasts were dissected from adjacent tissue using micro-dissection techniques. Since the initial dislocation of the incisor created a separation of fresh enamel organ tissue from enamel, the micro-dissection consisted only of gentle lifting of the freeze-dried enamel organ tissue from the enamel and severing it from alveolar bone with a fine instrument under a dissecting microscope. To localize the maturation stage of enamel formation, measurements were made from the growing tip based on the information derived from midsagittal sections of comparable rat incisors. The freeze-dried specimens were mounted on carbon studs and coated with carbon at a thickness of 20 nm. The surface morphology of ameloblasts was examined in a Cambridge Stereoscan S4-10 scanning electron microscope at 45° tilt angle and 20 kV. The surface of the enamel organ previously in contact with enamel was scanned for major regions of differing morphology. Fractures frequently occurred in the freeze-dried specimens parallel to the longitudinal axis of the ameloblasts which exposed their lateral surfaces. Separation along these fractures and examination of the lateral surfaces aided the identification of morphologic variations between major groups of cells from this perspective. The carbon-coated specimens were analyzed using an energy dispersive x-ray spectrometer (EDAX Model 707A) attached to the SEM. The operating conditions of the analyzer were 100 s for recording spectra at 20 kV and a beam size of approximately 100 nm. The spectra were recorded in the range of 0.0 - 8 keV with 20 eV per channel. The calcium peak was recorded at 3.700 keV. The net calcium counts per 100s and peak-to-background ratios, corrected after subtracting $K-K_B$ counts in each specimen were determined using a NOVA 3 computer run EDIT/EM 00219-91 program. A minimum of 10 readings were recorded for each region analysed in the nine rats investigated. Specimens from three rats could be analyzed in one day; thus the readings were combined into three groups, all of which were derived under identical conditions. The regions selected for microanalysis were proximal and distal ends of the lateral fractured surfaces of the two observed types of maturation ameloblasts. Both cellular and intercellular regions were included in each analysis since the analytical volume consisted of a surface area of 8 × 8 μm and an estimated depth of 10-15 μm. Since these cells are 40-50 μm in height, there was no difficulty in making separate proximal and distal analyses. The results were presented in the form of peak-to-background ratios as they are less sensitive to the surface roughness of the specimen (Roomans, 1988).

The data were statistically analyzed using the Student's t-test with a p value of 5% or less indicating a significant difference and a p-value of 1% or less indicating a highly significant difference.

In order to examine the morphology of the ameloblasts immediately after their mechanical separation from enamel, five additional rats were killed by ether overdose and their incisors were fixed by immersion in 2% glutaraldehyde containing 0.05M potassium pyroantimonate. The tissue blocks were rinsed and postfixed in 1% osmium tetroxide and routinely prepared for transmission electron microscopy (TEM).

In addition, two ether anesthetized rats were perfused intracardially with 2% glutaraldehyde and their lower incisors processed for light microscopy. This was to allow observation of basic morphologic differences in the maturation ameloblast types and the relative distribution of each along the length of the maturation enamel. Further, the light microscopic and TEM data were correlated with the SEM data to better characterize the type of maturation ameloblast observed by the latter. An additional advantage of the TEM data was to ensure that the SEM specimens were devoid of enamel crystals at the distal ends of the maturation ameloblasts which would compromise the calcium microanalysis.

Results

Light Microscopy

Light microscopic examination of semi-thin sagittal sections, cut parallel to the long axis of the rat incisor, revealed maturation enamel organ regions of ruffle-ended (RA) and smooth-ended (SA) ameloblasts (Fig. 1). The RA was clearly the predominant cell type. RA displayed distal ends consisting of a striated border and very limited intercellular spaces which were closed at the distal ends where the cells abut the surface of enamel. The distal regions of most SA were separated by wide intercellular spaces, many of which reached the enamel surface.

Scanning Electron Microscopy

The major components of the enamel organ, maturation ameloblasts and papillary cells could be readily recognized on the fractured lateral surfaces of the freeze-dried specimens. In most of the specimens, a clean separation had occurred between the distal ends of ameloblasts and the enamel (Fig. 2). Occasionally portions of the cell broke away and adhered to the enamel surface. In no instance was there any evidence of enamel crystals adhering to the cells. The lateral surfaces of the ameloblasts could be examined because of fractures in the specimens which occurred along the length of these cells (Fig. 3). The distal end-surfaces of the ameloblasts (previously facing enamel) displayed regions of two major variations in morphology,
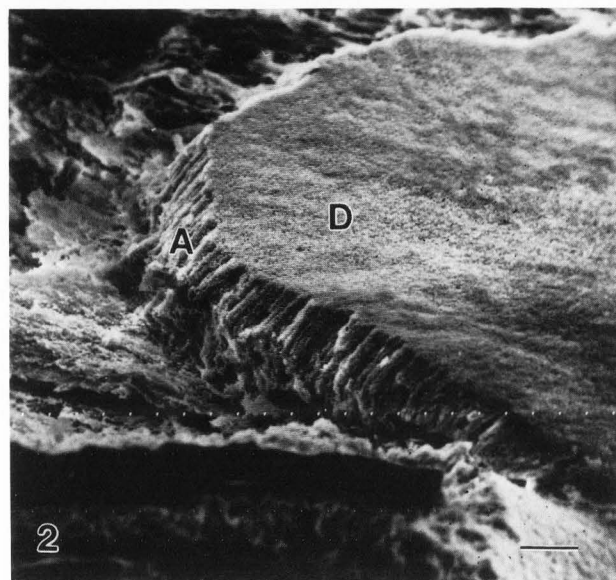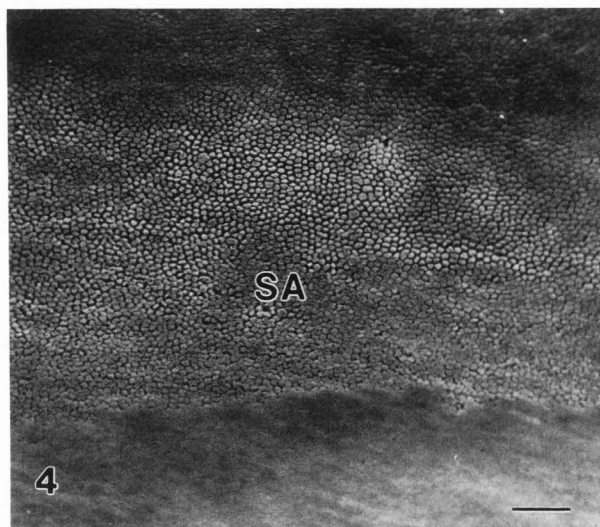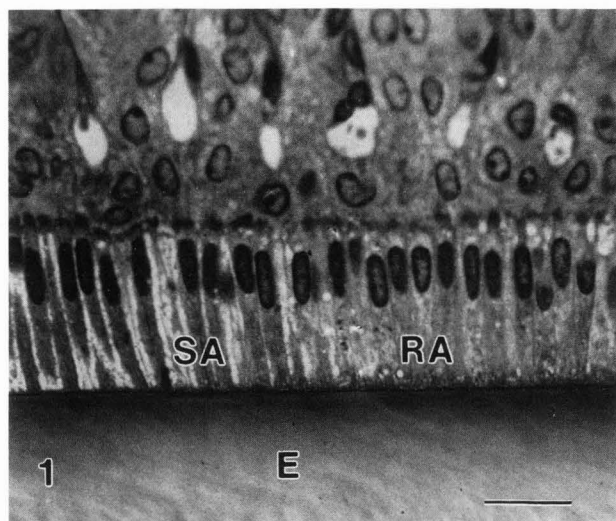
Fig. 1. Orientation light micrograph of maturation enamel (E) with regions of smooth-ended (SA) and ruffle-ended (RA) ameloblasts in the rat incisor. The SA are separated by wide intercellular spaces, many of which reach the enamel surface. Bar = 25 μm.

Fig. 2. Scanning electron micrograph of freeze-dried enamel organ tissue from the maturation zone. In the bulk of the specimen, separation occurred between the distal ends (D) of the ameloblasts (A) and the enamel surface when the incisor was manually dislocated from its socket just prior to freezing. Bar = 40 μm.
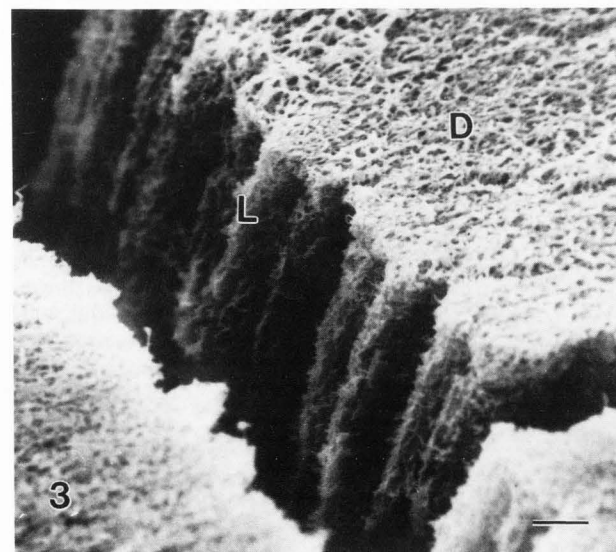
Fig. 3. Scanning electron micrograph showing higher power view of lateral and distal surfaces of maturation ameloblasts. Fractures commonly occurred during freeze-drying of the tissue block which permitted examination of the lateral surfaces of the cells. (D) Distal surface facing enamel and (L) lateral surface of cells. Bar = 5 μm.

Fig. 4. Scanning electron micrograph of distal surface of maturation ameloblasts displaying a frequently observed pattern of alternating bands of differing surface patterns. Note the wide intercellular spaces in the band which runs across the predominant portion of the micrograph and is considered representative of smooth-ended ameloblasts (SA). Bar = 40 μm.

presumed to represent the well known alternating bands of differing cell surface patterns of this tissue (Figs. 4 and 5). The two types of regions were further distinguished by examination of lateral ameloblast surfaces in fracture areas.

Two distinct morphologic patterns were observed in the lateral surfaces of maturation ameloblasts. In one the lateral surfaces were covered with microridges. In these regions the narrow intercellular spaces between ameloblasts were closed at their distal ends, (Fig. 6) which also displayed a microvillous configuration (Fig. 7). These cells were classified as ruffle-ended ameloblasts (RA). The second type of
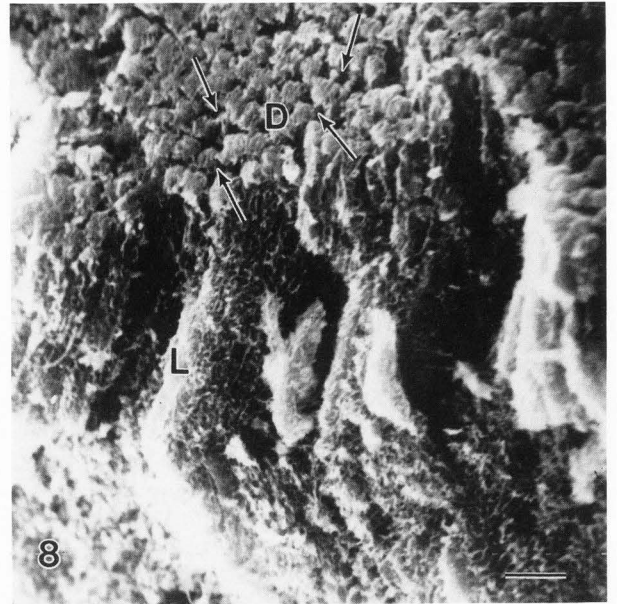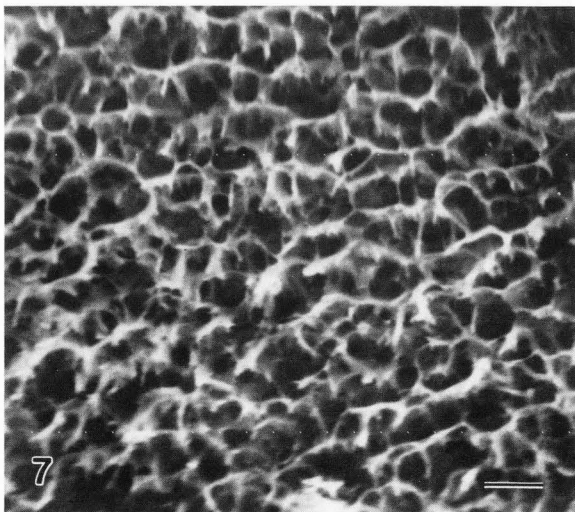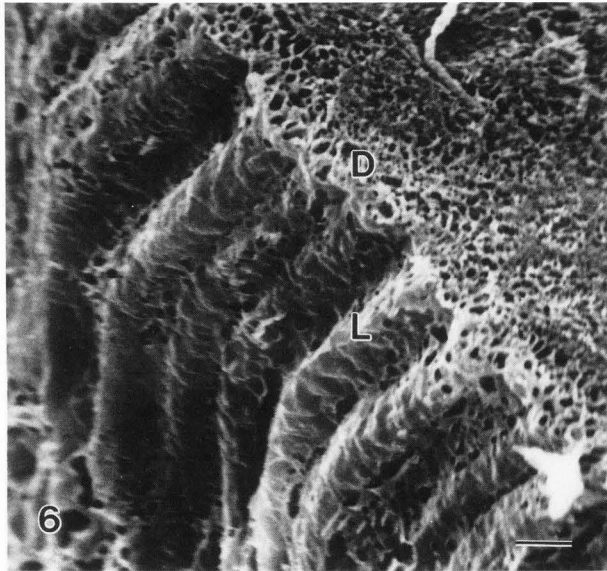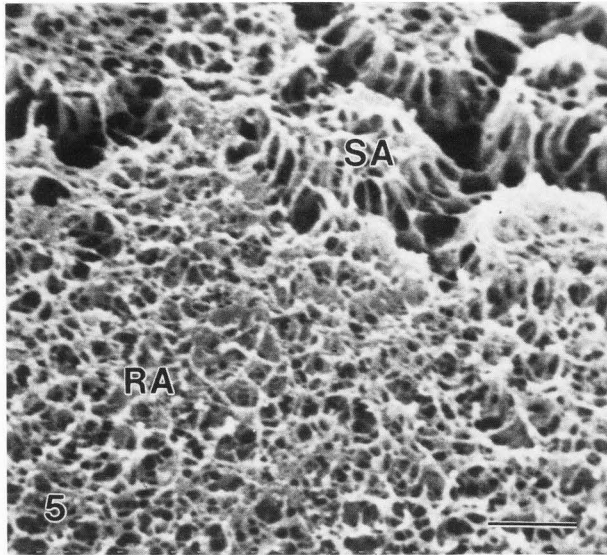
Fig. 5. High resolution scanning electron micrograph of area of transition between bands of maturation ameloblasts of differing surface patterns. Ameloblasts with wide extracellular spaces shown in upper part of the micrograph are identified as SA and those shown in the lower part as ruffle-ended ameloblasts (RA). Bar = 3 μm.

Fig. 6. Scanning micrograph of lateral surfaces (L) and distal ends (D) of cells identified as RA. The lateral surfaces are covered with microridges. Note that the intercellular spaces are quite limited and do not appear to be open to the enamel surface. Bar = 5 μm.

Fig. 7. Scanning electron micrograph of the freeze-dried enamel organ showing the distal surfaces of the RA. Note the microvillous configurations of the cellular surface facing the enamel. Bar = 5 μm..

Fig. 8. Scanning micrograph of lateral surfaces (L) and distal ends (D) of cells identified as SA. The lateral cell surfaces are of a maze configuration. The rather uniform distal ends of the cell bodies are separated by intercellular spaces which appear to be open to the enamel surface (arrows). Bar = 5 μm.

maturation ameloblasts which was much less common displayed wide intercellular spaces which were continuous and open at the enamel surface (Figs. 8 and 9). Their lateral cell surfaces were of a maze configuration (Fig. 8) and their distal ends did not possess microvilli. Such cells were identified as smooth-ended ameloblasts (SA).

Transmission Electron Microscopy

TEM examination of the tissue specimens preserved by glutaraldehyde immersion fixation immediately after mechanical separation verified that only soft tissues were included in the dissected enamel organ specimens. Figure 10 demonstrates the ultrastructure of maturation ameloblasts which had
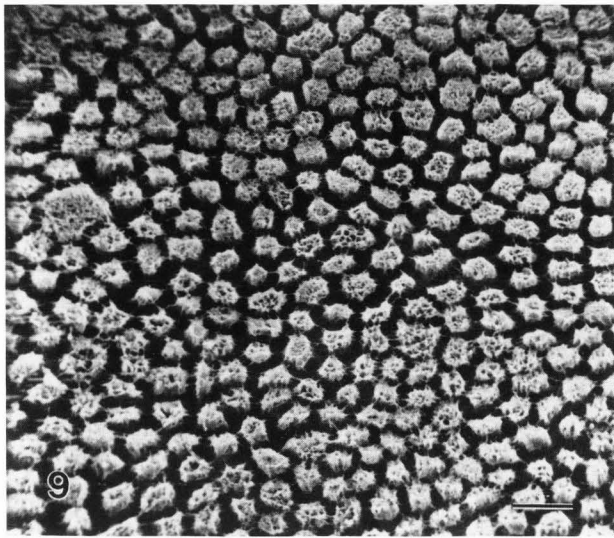
Fig. 9. Scanning micrograph of the distal surfaces of maturation ameloblasts in a band with wide intercellular spaces, identified as smooth-ended ameloblasts. Bar = 10 μm.
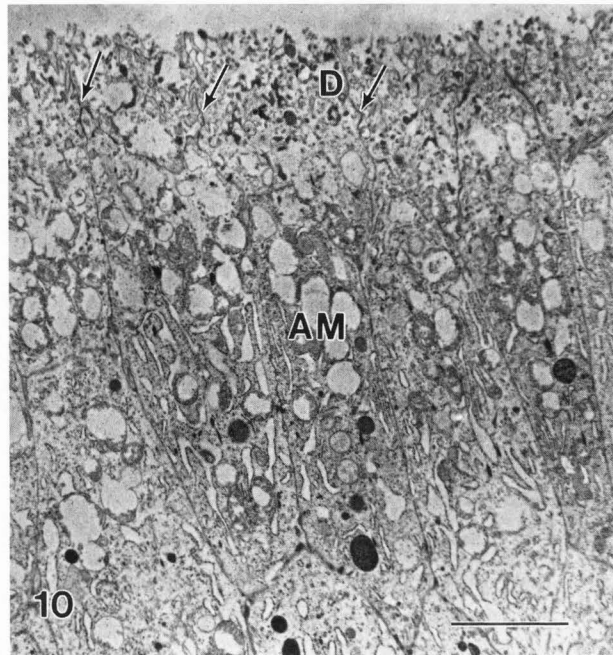
Fig. 10. Transmission electron micrograph of maturation ameloblasts of enamel organ fixed in glutaraldehyde immediately after mechanical separation from enamel. Note the absence of any vestiges of enamel at the distal surface. Distal end (D) of ameloblasts (AM) distal junctional complex (arrows). Bar = 5 μm.

Figs. 11 A,B. Spectra obtained by energy-dispersive x-ray spectrometric microanalysis of distal-lateral ends of the different maturation ameloblast regions of the freeze-dried enamel organ: (A) ruffle-ended (RA); and (B) smooth-ended (SA). Notice the high Ca peak in (A) and low Ca peak in (B).
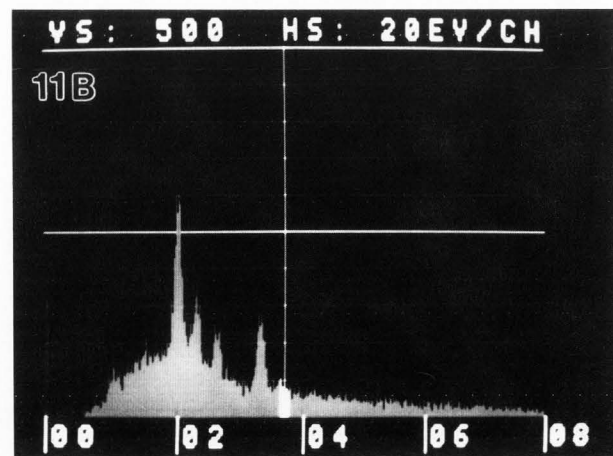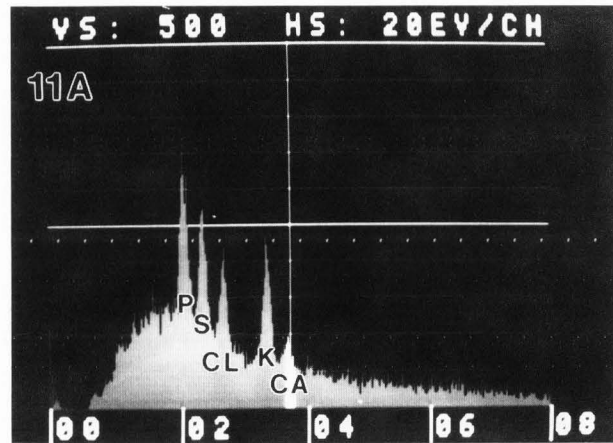
been separated from the enamel. It is clear that the mineralized enamel was left behind on the tooth surface as the separation appears to have occurred within the most distal cytoplasmic region such as the fragile ruffled border. Segments of the distal junctional complex are evident which indicates that only a small portion of the cell remained behind on the enamel surface.

Energy Dispersive X-Ray Spectometric Microanalysis

The microanalysis of calcium concentration along the lateral surfaces of the two morphologic types of ameloblasts was done at the distal and proximal zones. The representative x-ray spectra produced for the distal ends of cells identified as RA and SA are shown in Figs. 11A and 11B. The summary of all analyses is presented in Table 1. Comparison of calcium levels between the proximal portions of the lateral surfaces of the two cell types indicated no significant difference in calcium levels in RA and SA. Within the ruffle-ended type the distal regions (DL) showed higher calcium concentrations than the proximal (PL), whereas no significant difference was noted between DL and PL for

Ashrafi, S.H., Eisenmann, D.R. and Zaki, A.E.

Table 1. PEAK-TO-BACKGROUND P/B RATIOS (MEAN AND SEM) FOR CALCIUM LEVELS MEASURED AT THE PROXIMAL-LATERAL (P-L) AND DISTAL-LATERAL (D-L) SURFACES OF MATURATION AMELOBLASTS

Sample	Ruffle-Ended (RA)		Smooth-Ended (SA)	
	P-L ($\times 10^{-2}$)	D-L ($\times 10^{-2}$)	P-L ($\times 10^{-2}$)	D-L ($\times 10^{-2}$)
Group 1 (Mean ± SEM)	0.35 ± 0.08	0.55 ± 0.11	0.31 ± 0.07	0.22 ± 0.04
Group 2 (Mean ± SEM)	0.27 ± 0.05	0.43 ± 0.06	0.33 ± 0.04	0.27 ± 0.04
Group 3 (Mean ± SEM)	0.44 ± 0.02	0.62 ± 0.04	0.65 ± 0.03	0.39 ± 0.04
Means of Total P/B Ratios	0.36 ± 0.05	0.53 ± 0.05[1]	0.45 ± 0.08	0.31 ± 0.04[2]

[1] Differences between total P/B ratios of RA (P-L) and RA (D-L) are significant at $p < 0.05$.
[2] Differences between P/B ratios of RA (D-L) and SA (D-L) are significant at $p < 0.01$.

Note: Each group included specimens from three animals which were analysed at one time.

the SA. When calcium levels were compared between distal portions of the lateral surfaces of the two cell types, significantly higher levels were found in the ruffle-ended ameloblasts than the smooth-ended ones.

Discussion

Rapid freezing of mechanically dislocated enamel organ preserved morphological features of the maturation ameloblasts sufficiently to characterize two types of cells. The distinguishing features (intercellular space and configuration of the lateral surfaces and distal ends of the cells) corresponded with observations reported earlier by Reith (1970), Warshawsky and Smith (1974) and Nishikawa and Josephsen (1987) using light microscopy and Boyde and Reith (1976, 1977) and Skobe et al. (1985, 1988), using scanning electron microscopy. Regions of SA were observed infrequently, which correlates with a report of their constituting approximately 16% of the full length of rat incisor maturation ameloblasts (Smith et al., 1987). The ability to recognize regions identified as SA and RA in our specimens permitted comparison of calcium concentrations in various regions of these two representative cell types.

The absence of any trace of enamel crystals at the distal ends of the cells (as observed by TEM) gave assurance that the element counts in the analytical spectra were indeed derived from the cells and not from extraneous mineral sources. Inevitably some damage occurred to the distal ends of the maturation ameloblasts during mechanical separation. However, there is a distinct advantage to having only the cellular

material under the analytical beam to insure that no artifactual element counts are picked up from the mineralized enamel. In RA the separation appeared to occur near the distal extremity of the fine membranous network making up the ruffled border. Intact distal junctions observed with TEM correlated with the SEM appearance of close apposition of the distal ends of these cells.

The previously reported banded pattern of enamel maturation appears to be closely related to activities of the adjacent cyclic ameloblasts. This may be accomplished by cellular influence over calcium transport (Reith and Boyde, 1981; Crenshaw and Takano, 1982) or over certain constituents of the organic matrix in the adjacent enamel surface, which also reflect the alternating pattern of RA and SA (Mckee and Warshawsky, 1986). Attention has been focused on control by the cells through factors such as permeability of junctions, distribution of ion transport enzymes and organelles and localization of cell associated calcium.

Various investigators using horseradish peroxidase (Takano and Ozawa, 1980; Kallenbach, 1980) and lanthanum (Takano and Crenshaw, 1980) have found that whereas diffusion of tracers through the SA layer occurs readily, it is inhibited by tight intercellular junctions at the distal ends of RA. Thus it has been assumed that transport of calcium through the RA layer is an active transcellular process. However, it should also be mentioned that this assumption is somewhat difficult to reconcile with the fact that calcium moves very rapidly through the maturation enamel organ into adjacent enamel

(Hammarstrom, 1967; Munhoz and Leblond, 1974; Bawden and Wennberg, 1977; Reith et al., 1984; Eisenmann et al., 1989).

Evidence of an ATP-dependent calcium pump as a factor in active calcium transport by ameloblasts has been produced in recent years. Ca^{2+}- Mg^{2+} ATPase has been demonstrated cytochemically in association with the entire cell membrane of secretory ameloblasts (Inage and Weinstock, 1979; Sasaki and Garant, 1986; Takano et al., 1986) and localized particularly along the ruffled border of ruffle-ended maturation ameloblasts (Salama et al., 1987; Takano and Akai, 1987). It is also noteworthy that calcium uptake by enamel regions corresponding with ruffle-ended maturation ameloblasts was greatly decreased when vanadate, a Ca^{2+}-ATPase inhibitor was introduced (Takano et al., 1987).

It has been difficult to clarify the distribution and levels of calcium in association with various components of the maturation ameloblasts. This is due primarily to the lability of this ion and its susceptibility to translocation or loss during tissue preparation. Early energy dispersive x-ray spectrometry studies of frozen tissues produced mixed results. Boyde and Reith (1978) found very low levels of calcium in both secretory and maturation rat incisor ameloblasts, whereas Engel (1981), in a study of mouse molars, demonstrated a five-fold increase in concentration of calcium in ameloblasts from the secretory to the maturation stage. A more recent investigation using autoradiography and energy dispersive x-ray spectometry of frozen tissues also found differences in calcium levels in the various cell layers of the enamel organ of the rat incisor (Kawamoto and Shimizu, 1987). Both methods employed revealed higher concentrations of calcium in maturation ameloblasts than secretory ameloblasts. A gradient of increased calcium concentration from the proximal to the distal ends of the maturation ameloblasts was observed. Although these authors reported no attempt to distinguish the two types of maturation ameloblasts, it is very likely that most of their readings were from ruffle-ended cells due to their predominance.

Utilizing potassium pyroantimonate cytochemistry, Kogaya and Furuhashi (1988) recently demonstrated heavy calcium labelling of mitochondria and the plasma membrane (particularly the ruffled border) of RA in chemically preserved rat incisors. They found no specific localization pattern in SA.

In another recent report, Takano et al. (1988) demonstrated calcium localization within rapidly frozen maturation ameloblasts by the GBHA staining method. Mitochondria, tubulo-vesicular structures and the ruffled border appeared to be most reactive. Both SA and RA showed substantial GBHA reaction, but the heaviest localized region appeared to be the distal ends of the RA.

In summary, the greater body of evidence appears to support increased calcium activity toward the distal pole of ruffle-ended ameloblasts, which may involve the cell membrane of the ruffled border and its associated ion transport enzymes as well as mitochondria and other related organelles.

The calcium gradient from proximal to distal found in RA in the present study correlates well with these recent reports of other investigators. Likewise the significantly higher levels in the distal RA as compared to the distal SA correspond with the commonly reported cyclic pattern of calcium incorporation of enamel. These results and those of other authors cited lend support for an active role for maturation ameloblasts in control of movement of calcium to the enamel front.

Acknowledgments

References

Ashrafi SH, Eisenmann DR, Zaki AE (1987) Secretory ameloblasts and calcium distribution during normal and experimentally altered mineralization. Scanning Microscopy 1: 1949-1962.

Bawden JW, Wennberg A (1977) In vitro study of cellular influence on ^{45}Ca uptake in developing rat enamel. J. Dent. Res. 56: 313-319.

Boyde A, Reith EJ (1976) Scanning electron microscopy of the lateral cell surfaces of rat incisor ameloblasts. J. Anat. 122: 603-610.

Boyde A, Reith EJ (1977) Scanning electron microscopy of rat maturation ameloblasts. Cell Tiss. Res. 178: 221-228.

Boyde A, Reith EJ (1978) Electron probe analysis of maturation ameloblasts of the rat incisor and calf molar. Histochemistry 55: 41-48.

Crenshaw MA, Takano Y (1982) Mechanisms by which the enamel organ controls calcium entry into developing enamel. J. Dent. Res. 61: 1574-1579.

Eisenmann DR, Ashrafi SH, Zaki AE (1982) Multi-method analysis of calcium localization in the secretory ameloblasts. J. Dent. Res. 61: 1555-1561.

Eisenmann DR, Ashrafi SH, Zaki AE (1984) Calcium distribution in freeze-dried enamel organ tissue during normal and altered enamel mineralization. Calcif. Tissue Int. 36: 596-603.

Eisenmann DR, Chen J, Lehman G, Zaki AE (1989) Studies on the influx of ^{3}H-histidine and ^{45}Ca through a surgical opening to rat incisor ameloblasts and adjacent enamel. Archs. Oral Biol. 34: 93-102.

Engel MB (1981) Microprobe analysis of calcifying matrices and formative cells in developing mouse molars. Histochemistry 72: 443-452.

Hammarstrom L (1967) Different localization of tetracycline and simultaneously injected radiocalcium in developing enamel. Calcif. Tiss. Res. 1: 229-242.

Inage T, Weinstock A (1979) Localization of the enzyme ATPase in the rat secretory ameloblasts by means of electron microscopy. J. Dent. Res. 58(B): 1010.

Josephsen K, Fejerskov O (1977) Ameloblast modulation in the maturation zone of the rat incisor enamel organ: A light and electron microscopic study. J. Anat. 124: 45-70.

Kallenbach E (1980) Access of horseradish peroxidase to the extracellular spaces of the maturation zone of the rat incisor enamel organ. Tiss. Cell. 12: 165-174.

Kawamoto T, Shimuzu M (1987) Distribution of calcium and phosphate in cells of the enamel organ in the rat lower incisor. Adv. Dent. Res. 1: 236-244.

Kogaya Y, Furuhashi K (1988) Comparison of the calcium distribution pattern among several kinds of hard tissue forming cells of some living vertebrates. Scanning Microscopy 2: 2029-2043.

McKee MD, Warshawsky H (1986) Effects of various agents on staining of the maturation pattern at the surface of rat incisor enamel. Archs Oral Biol. 31: 577-585.

McKee MD, Warshawsky H, Nanci A (1987) Use of backscattered electron imaging on developed radioautographic emulsions: Application to viewing rat incisor enamel maturation pattern following [45]calcium injection. J. Electron Micros. Tech. 5: 357-365.

Munhoz COG, Leblond CP (1974) Deposition of calcium phosphate into dentin and enamel as shown by radioautography of sections of incisor teeth following injection of [45]Ca into rats. Calcif. Tiss. Res. 15: 221-235.

Nishikawa S, Josephsen K (1987) Cyclic localization of actin and its relationship to junctional complexes in maturation ameloblasts of the rat incisor. Anat. Rec. 219: 21-31.

Reith EJ, Cotty VF (1962) The absorptive activity of ameloblasts during the maturation of enamel. Anat. Rec. 157: 577-588.

Reith EJ (1970) The stages of amelogenesis as observed in molar teeth of young rats. J. Ultrastruct. Res. 30: 111-151.

Reith EJ, Boyde A (1981) Autoradiographic evidence of cyclical entry of calcium into maturing enamel of the rat incisor tooth. Archs Oral Biol. 26: 983-987.

Reith EJ, Boyde A, Schmid MI (1982) Correlation of rat incisor ameloblasts with maturation cycles as displayed on enamel surface with EDTA. J. Dent. Res. 61: 1563-1573.

Reith EJ (1983) A model for transcellular transport of calcium based on membrane fluidity and movement of calcium carriers within the more fluid microdomains of the plasma membrane. Calcif. Tissue Int. 129: 134.

Reith EJ, Schmid MI, Boyde A (1984) Rapid uptake of calcium in maturing enamel of the rat incisor. Histochemistry 80: 409-410.

Reith EJ, Boyde A (1985) The pyroantimonate reaction and transcellular transport of calcium in rat molar enamel organs. Histochemistry 83: 539-543.

Robinson C, Briggs HD, Atkinson PJ, Weatherell JA (1979) Matrix and mineral changes in developing enamel. J. Dent. Res. 58(B): 871-880.

Roomans GM (1988) Quantitative x-ray microanalysis of biological specimens. J. Electron Microsc. Tech. 9 :19-43.

Salama AH, Zaki AE, Eisenmann DR (1987) Cytochemical localization of Ca^{2+}-Mg^{2+} adenosine triphosphatase in rat incisor ameloblasts during enamel secretion and maturation. J. Histochem. and Cytochem. 35: 471-482.

Sasaki T, Garant PR (1986) Ultracytochemical demonstration of ATP- dependent calcium pump in ameloblasts of rat incisor enamel organ. Calcif. Tissue Int. 39: 86-96.

Skobe Z, Lafrazia F, Prostak K (1985) Correlation of apical and lateral membrane modulations of maturation ameloblasts. J. Dent. Res. 64: 1055-l061.

Skobe Z, Prostak KS, Stern DN (1988) A scanning electron microscope study of monkey maturation-stage ameloblasts. J. Dent. Res. 67: 1396-1401.

Smith CE, McKee MD, Nanci A (l987) Cyclic induction and rapid movement of sequential waves of new smooth-ended ameloblast modulation bands in rat incisors as visualized by polychrome fluorescent labeling and GBHA-staining of maturing enamel. Adv. Dent. Res. 1(2): 162-175.

Suga A (1959) Amelogenesis, some histological and histochemical observations. Int. Dent. J. 9: 394-420.

Takano Y, Akai M (1987) Demonstration of Ca^{2+}-ATPase activity in the maturation ameloblast of rat incisor after vascular perfusion. J. Electron Microsc. 36: 196-203.

Takano Y, Crenshaw MA (1980) The penetration of intravascularly perfused lanthanum into the ameloblast layer of developing rat molar teeth. Archs Oral Biol. 25: 505-511.

Takano Y, Ozawa H (1980) Ultrastructural and cytochemical observations on the alternating morphologic changes of the ameloblasts at the stage of enamel maturation. Arch Histol. Jpn. 43: 385-399.

Takano Y, Crenshaw MA, Bawden JW, Hammarstrom L, Lindskog S (1982) The visualization of the patterns of ameloblast modulation by the Glyoxy Bis (2-hydroxyanil) staining method. J. Dent. Res. 61: 1580-1586.

Takano Y, Ozawa H, Crenshaw MA (1986) Ca-ATPase and ALPase activities at the initial calcification sites of dentin and enamel in the rat incisor. Cell Tissue Res. 243: 91-96.

Takano Y, Matsuo S, Wakisaka S, Ichikawa H, Nishikawa S, Akai M (1987) The influence of vanadate on calcium uptake in maturing enamel of the rat incisor. J. Dent. Res. 66: 1702-1707.

Takano Y, Matsuo S, Wakisaka S, Ichikawa H, Nishikawa S, Akai M (1988) A histochemical demonstration of calcium in the maturation stage enamel organ of rat incisors. Arch. Histol. Cytol. 51: 241-248.

Taylor AN (1984) Tooth formation and the 28,000-dalton vitamin D-dependent calcium-binding protein: an immunocytochemical study. J. Histochem. Cytochem. 32: 159-164.

Warshawsky H, Smith CE (1974) Morphological classification of rat incisor ameloblasts. Anat. Rec. 179: 423-466.

Discussion with Reviewers

J. Appleton: I do not think it is scientifically sound to use a TEM method involving aqueous fixation to determine the presence or absence of calcium in SEM specimens prepared by an entirely different method.
Authors: The TEM method was used only to show the condition of the distal ends of the ameloblasts following separation from the enamel surface. Only freeze-dried SEM specimens were used for calcium analysis.

J. Appleton: The freeze drying technique you use will undoubtedly produce considerable morphological damage to the ameloblast since at -35°C there will be ice crystal growth as the specimen warms up from -150°C. Is this not also going to produce intracellular shifts of calcium ions?
Authors: Ice crystal growth and some shifting of calcium ions no doubt occur. It is important to note that relatively large tissue areas are being analysed which include both intracellular and intercellular regions in each analytical volume. It is expected that the shifting of calcium ions occurs over much shorter distances than that which is encompassed by the areas of analysis from which the readings were taken.

J. Appleton: The extracellular environment of the ameloblasts probably contains calcium ions in a concentration at least a thousand times higher than the intracellular concentration. With this in mind how do you suggest that the ameloblast regulates the passage of calcium ions in the enamel?
Authors: Due to the metabolic requirement of maintaining low cytosolic calcium levels in cells, it is most likely that the vast majority of the calcium in this tissue is in the intercellular region or in association with cell membranes. It is suggested that cellular regulation occurs predominantly by means of transport enzymes, calcium binding proteins or intrinsic membrane components all of which are associated with the cell membrane. Regulation by organelles or cytosolic components would be expected to play a lesser role.

G.M. Roomans: Why was potassium pyroantimonate added to the fixative? No comments are made about calcium precipitates in the ameloblasts.
Authors: Potassium pyroantimonate was not used to localize calcium precipitates in the ameloblasts in this study. Only freeze-dried bulk specimens, prepared by the SEM method, were used to determine calcium levels by energy dispersive x-ray microanalysis.

G.M. Roomans: From Figs. 11A and B it appears that there were not only differences in calcium, but also in other elements. Were data about the other elements collected and can you comment on the biological significance of these data?
Authors: Study of the other elements is in progress.

Y. Takano: Kashiwa KH and Atkinson WB (The applicability of a new Schiff base, glyoxal bis (2-hyroxy-anil) for the cytochemical localization of ionic calcium. J. Histochem. Cytochem., 11:258-264, 1963) pointed out that during freeze drying of the rapidly frozen tissues, the temperature should be below the eutectic point of calcium chloride (-54.9°C) to prevent the false localization of calcium ions. The temperature used in this study for freeze drying (-35°C) was well above the eutectic point of calcium chloride. I want to hear the authors'comment on this serious problem.
Authors: The use of isopentane is always regarded as superior to direct liquid nitrogen freezing because of the vaporization of the latter which can delay freezing and produce more ice crystals. In our method the tissue is frozen at -150°C and is never subsequently melted. It is only an assertion that the eutectic point of calcium chloride would have any bearing on the result of sublimation of water vapor from the specimen since the chemical form of the calcium in the tissues is not known. Very likely, most of the calcium is in association with various organic molecules.

Y. Takano: Table 1 does not provide any information as regards the difference in quantity of calcium ions in the ameloblasts between early and late stages of enamel maturation. Did you find any difference?
Authors: Only tissue from early maturation was examined.

Z. Skobe: Figure 10 demonstrates that apical portions of the cells were broken off (and adhered to the enamel). That is understandable since it is very difficult to remove maturation stage ameloblasts from the nascent enamel. Figures 5, 6, and 7 are further examples of cells with apical portions missing. Should you not just seek out those few areas as in Figure 4, where you are sure of what you are seeing and where you are taking counts?
Authors: Lower magnification views of large surface areas (as illustrated in Fig. 4) were most useful in identifying alternating bands of differing cell surface patterns. The two types of regions were then further distinguished by examination of lateral ameloblast surfaces in fracture areas. Although it is evident that apical (distal) portions of the cells were broken off, the presence of distal junctional complexes (Fig. 10) indicates that only a small portion of the cells remained behind on the enamel surface.

Z. Skobe: I have no idea what the groups are in Table 1, but there is a significant difference between the groups in the RA region, what does that mean?
Authors: Specimens from three animals could be analyzed in one day; thus the readings were combined into three groups. Since all of the readings were derived under identical conditions, there is no known significance to differences between the groups other than usual specimen variations.

Reviewer V: It has been shown that in enamel, supersaturation during freezing concentrates solutes into water droplets that become artefactual granules. Under the conditions used, the calcium aggregates formed in the intercellular fluid would cling to the cell membrane. Thus, a greater surface area provided by cell ruffling would provide for a greater capacity to

Ashrafi, S.H., Eisenmann, D.R. and Zaki, A.E.

bind the artifactual particles. The present results therefore merely report the fortuitous distribution of calcium under these circumstances. Please comment.

Authors: Ice crystals in such freeze-dried soft tissues are typically 0.1-0.5 μm in diameter (Boyde A and Reith EJ, Qualitative Electron Probe Analysis of Secretory Ameloblasts and Odontoblasts in the Rat Incisor, Histochemistry 50:347-354, 1977) whereas the microanalytical area used in our investigation is 8 × 8 μm with a spatial resolution (depth of beam penetration) of 10 μm. The contention that our results are affected by having more calcium aggregates formed in the intercellular fluid and adsorbed to a greater surface area of ruffled membranes is negated by the fact that intercellular regions, cells and their membranes are all included in the analytical area. It should be emphasized that the results refer to detectable calcium in the analytical area and do not specify a specific cellular or intercellular site. Equally important is that the procedure followed provided for prompt, clean separation of cellular material from the adjacent mineralizing enamel, where a larger reservoir of calcium might be drawn upon. In addition, transmission electron microscopy of the specimens utilized for analysis revealed that a portion of the ruffled-membrane is left behind on the enamel, which greatly reduces the likelihood that increased membrane surface area alone is responsible for higher calcium readings.